VOLUMEN 48
XXXI Verano De la Ciencia
ISSN 2395-9797
www.jovenesenlaciencia.ugto.mx

Search for double-lined spectroscopic binary stars

Búsqueda de estrellas binarias espectroscópicas con líneas doble

Marco Aleajndro Anaya Guerrero[1], Dennis Jack[2]
[1]División de Ciencias e Ingenierías (DCI), Universidad de Guanajuato.
ma.anayaguerrero@ugto.mx
[2]Departamento de Astronomía, División de Ciencias Naturales y Exactas, Universidad de Guanajuato.
dennis.jack@ugto.mx

Abstract

Detecting secondary stars in binary systems is challenging due to the stronger brightness of the primary star. In this study, we present a search for double-lined spectroscopic binary (SB2) stars by analyzing high-resolution spectra taken by the TIGRE telescope for 39 already known SB1 systems. We successfully detected the secondary star in HD 99797 using Cross-Correlation Function (CCF) profiles for the radial velocity. Although absolute precision was limited by instrumental scatter and the lack of available spectra, we constrained the secondary's radial velocity to a range between 20.01 km s^{-1} and 30.20 km s^{-1}. These findings provide a starting point for future monitoring and advanced radial velocity curve modeling.

Keywords: spectroscopic binaries; radial velocities; spectroscopy; individual star: HD 99797

Introduction

In the universe, binary star systems are very common. At least half of all stars in the sky are actually multiple systems, with two or more stars in orbit around a common center of mass (Carroll, 2014). The brighter star is called the primary, and the companion is considered the secondary. Although these objects are far away and are difficult to observe, there are a variety of methods to detect them and to obtain their orbital parameters. The classification of binary stars depends on how they are detected. One class is all spectroscopic binaries that are detected and studied by spectral line movement or the Doppler effect in the spectrum of the star. The light shifts to the blue when the star moves towards us, and it shifts to the red when it moves away from us. In some spectroscopic binaries, the spectral lines of both stars are visible, and the lines alternate between double and blended single. These are called double-lined spectroscopic binaries (SB2). In other systems, the spectrum of only one star is observed. This is called a single-lined spectroscopic binary (SB1)(Pattnaik *et al.,* 2011). Another type of binary star is eclipsing binary stars. In these systems, the orbital plane is aligned with the line of sight of the observer. They are studied by their light curve, which is characterized by almost constant brightness, with periodic drops in intensity when one star moves in front of the other star.

A challenge of studying these systems is to know the properties of the secondary star, because the light of the primary star outshines its presence. The study of these objects has recently become a focus of attention because recent technology allows the observation and detection of these types of systems much more easily. Over the years, different types of missions were developed with these goals. One of them is eROSITA (extended ROentgen Survey with an Imaging Telescope Array), which is a wide-field X-ray telescope on-board the Russian-German "Spectrum-Roentgen-Gamma" (SRG) observatory. Its main objective is the detection of very large samples, giving information about the spectra of objects in its detection range (Predehl *et al.,* 2021). On the other hand, there is Gaia, an astrometry space mission of the European Space Agency (ESA). It seeks to identify and investigate nearby stars, mapping the whole sky. Just like eROSITA, it has a database of identified stars for public study (Prusti *et al.,* 2016). The database is necessary to collect information and the characterizations of our candidate stars.

One problem in the study of celestial bodies in modern astrophysics is the saturation of information and available data. In the Astronomy Department at the Universidad de Guanajuato, we have the Telescopio Internacional de Guanajuato Robótico Espectroscópico (TIGRE), a telescope that allows us to target objects of interest and study their spectra with quite high resolution. The main objective of this work is to study binary

systems, using high-resolution spectra from the TIGRE telescope to determine if it is possible to detect double spectral lines (Schmitt *et al.,* 2014).

Binary Stars

General Information

We selected 39 target stars from a series of observations that detected bright SB1 spectroscopic binaries. These have been published based on their orbital periods: shorter than 365 days (Jack *et al.,* 2020), around 400 days (Jack *et al.,* 2022), longer than 500 days (Jack *et al.,* 2024), and up to 1000 days (Jack *et al.,* 2026).

For each binary system, we collected the parallax, radial velocity (Vrad), and brightness (Gm), along with their uncertainties. This information is very useful to understand the primary star and get an idea of how the whole system behaves. In Gaia, we revised data within a 5-arcsecond radius to look for any possible closely bound object, even though it is rare to clearly see the secondary star in these datasets (Vallenari *et al.,* 2023).

Finally, we checked and confirmed the information of our binary stars using the SIMBAD database (Wenger *et al.,* 2000). We also looked for additional data about the close environment and the secondary star using the eROSITA.DE Data Archive (Merloni *et al.,* 2024) and ROSAT (Voges *et al.,* 1999).

Spectra and radial velocity

The sample of stars was studied using TIGRE, a 1.2 m telescope connected to a fiber-fed échelle spectrograph. The instrument covers wavelengths between 3800 and 8800 Å with a resolving power above 20,000, although a gap of about 130 Å is present around 5800 Å (Schmitt *et al.,* 2014). Throughout the established observation periods, we monitored the spectra obtained for each star. By having spectral data in the red (5800 to 8800 Å) and blue regions (3800 to 5800 Å), we analyzed the stars with more precision.

With the help of the published SB1 orbital parameters, the obtained radial velocity (Vrad) curves of the stars allowed us to determine the exact times where there is a maximum or minimum. These are the most important points because that is when the stars reach their maximum or minimum Doppler shift. Consequently, the spectra of each star are shifted the most to the blue or red, respectively, showing their maximum spectral line separation.

Using the observed spectra and radial velocity curves, we analyzed each system to try to isolate the signal of the secondary star. The spectral analysis was performed using the latest version of the open-source framework iSpec (Blanco-Cuaresma, 2019; Blanco-Cuaresma *et al.,* 2014). This tool allowed us to analyze the observations on a spectrum-by-spectrum basis by computing the Cross-Correlation Function (CCF), mapping relative intensity against radial velocity (Vrad). Analyzing these CCF profiles facilitated the detection of the spectral signatures corresponding to the secondary component. Furthermore, we co-added the spectra at specific orbital phases of interest to increase the signal-to-noise ratio (S/N) and enhance the stellar features. Finally, the iSpec fitting module provided not only the Vrad measurements but also their associated uncertainties and the Gaussian dispersion or Full Width at Half Maximum (FWHM), which characterizes the spectral line broadening.

Principal Properties

Table 1 presents the basic information of the stars of our sample, including the name of the star, radial velocity (Vrad), and parallax with their respective errors, as well as the brightness in the Gaia G band (Gm). At this stage, our goal was simply to establish the foundational properties of the binary systems and understand the main characteristics of the primary stars measured.

Table 1. *Astrometric and kinetic parameters of 39 stars sample.*

Star	parallax (mas)	Vrad (km s^{-1})	Gm(mag)
HD 1585	2.8742±0.2076	38.7742±1.6012	6.2395
HD 6613	3.3490±0.1357	9.6264±1.5357	6.7448
HD12390	2.6610±0.0982	-12.0741±2.3284	6.2241
HD18665	2.7125±0.1263	-2.9126±1.8174	6.7169
HD 20656	4.2298±0.0508	7.7168±7.0503	6.8343
HD 27131	4.4019±0.0469	14.0994±4.6481	6.7049
HD 27259	3.4007±0.0508	2.6027±2.6713	6.9185
HD 39923	2.7673±0.3325	11.2212±2.1779	6.9999
HD 55201	5.5794±0.1716	51.4505±2.3400	6.9967
HD 98812	2.0380±0.0452	-33.3260±2.5510	6.9440
HD 147430	3.5923±0.1184	-35.6639±1.6320	6.4923
HD 150600	8.4370±0.1142	-7.4984±1.6882	6.9171
HD 171852	10.8966±0.0849	-28.2866±3.8477	6.3687
HD 193082	3.6804±0.0324	-88.5415±1.8945	6.9231
HD 195543	2.0876±0.0610	-19.3948±1.7287	6.9114
HD 202699	3.0198±0.1047	-15.0234±2.0337	6.5423
HD 215550	3.0779±0.0929	-3.5625±4.7927	6.9849
HD 217427	3.7644±0.0936	-24.8129±2.5517	6.3634
HD 221643	2.2828±0.1286	-3.7084±2.5594	6.4114
HD 9728	9.8819±0.1788	-12.1575±0.9939	6.2458
HD 12736	4.8319±0.1250	36.1688±1.5186	6.7981
HD 21835	4.0279±0.0973	-3.1531±1.1669	6.9530
HD 32575	5.4130±0.1466	-44.0844±1.1713	6.9008
HD 37698	4.4463±0.0586	20.0740±0.6774	6.5445
HD 40006	0.9929±0.0565	-1.5565±1.5324	6.9174
HD 41118	2.7455±0.1175	55.1773±1.3678	6.6744
HD 59539	2.4605±0.1190	1.3338±1.1751	6.2706
HD 80116	1.8661±0.1054	-0.5905±1.1480	6.6227
HD 88748	2.7780±0.0521	0.5233±1.1055	6.6154
HD 96778	6.0203±0.1579	-6.4517±0.8510	6.8744

HD 99797	15.8634±0.2157	16.0761±0.5535	6.8716
HD 121862	4.5318±0.0768	-7.9041±0.6917	6.8447
HD 148434	7.5732±0.0312	-5.3560±0.8457	6.6039
HD 172470	2.1096±0.0365	-12.3321±0.9364	6.5228
HD 177698	3.6061±0.0806	-35.9151±1.0286	6.7728
HD 189985	5.1641±0.0841	10.8419±1.5067	6.2757
HD 209615	6.5686±0.2683	-4.8859±1.2927	6.6665
HD 210075	5.4836±0.2907	-10.9238±1.5366	6.8606
HD 224673	2.2106±0.0796	5.9990±1.5506	6.2986

The data obtained from Gaia (Vallenari *et al.,* 2023) and SIMBAD (Wenger *et al.,* 2000) allowed us to gain a broad overview of our star sample, and to check if there is a possible detection of a secondary star at a close-by position. Table 2 shows that three stars have detection of close-by objects within 5 arcseconds. However, all these are to faint to be actual secondary stars in the bright binary systems. Additionally, using catalogs from eROSITA (Merloni *et al.,* 2024) and ROSAT (Voges *et al.,* 1999), we collected information regarding X-ray measurements from a possible interaction between the primary and the secondary star, like mass overflow. We found four stars with X-ray detections (see Table 3). However, X-ray detection can also come from stellar activity, and further studies are necessary to determine the origin of the detected X-ray emission.

Table 2. *Stars detected close to the primary stars position with their properties (Gaia).*

Star	*Close-by object*	*(mas)*	*Gm(mag)*
HD195543	HD 195543	2.5507±0.0232	12.0991
HD 32575	HD 32575	_	17.4227
HD 189985	HD 189985	_	17.7824

Table 3. *X-ray detection at the primary star position and their properties (eROSITA).*

Star	*eROSITA detection*	*Counts*	*ROSAT detection*	*Counts*
HD 27131	1eRASS J041711.0+050128	27.7	_	_
HD 96778	1eRASS J110902.4+300225	41.2	2RXS J110903.1+300234	16.99
HD 99797	1eRASS J112859.0+100216	7.7	2RXS J112858.9+100211	20.3
HD 121862	1eRASS J135757.2+050707	7.1	_	_

Spectra and Vrad analysis

Subsequently, we analyzed the radial velocity curves of our sample. These curves are fundamental because they allowed us to determine the orbital period of each binary system and precisely locate their points of maximum and minimum radial velocity. It is exactly at these extremes of the curve where the Doppler effect is strongest, meaning the spectral lines reach their maximum shift towards the red (when the star is receding)

and towards the blue (when it is approaching). A possible secondary star has the opposite Doppler effect and the lines are the most separated.

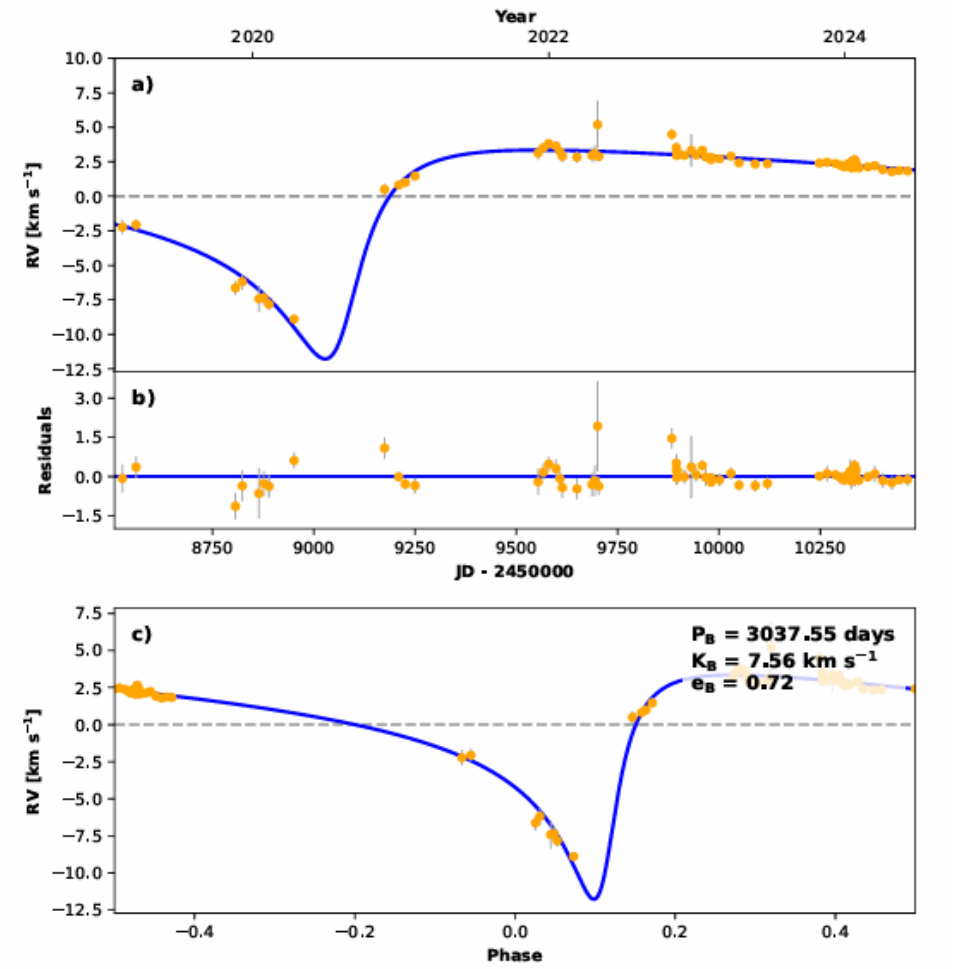

Figure 1. Radial velocity of HD 99797, measured in the years 2018-2024.

The maximum and minimum points of the radial velocity curve make it much easier to analyze the spectra. Using iSpec (Blanco-Cuaresma, 2019), we analyzed the observations exactly at these points, which is precisely when we can most clearly perceive the different lines in the spectral band. As shown for example in Figure 2, we visualized these data by plotting the velocity on the x-axis and the relative intensity on the y-axis.

We found only one positive detection in the sample of 39 stars. In Figure 1, where we analyzed the system's movement of the star HD 99797, we observed that the radial velocity reaches its minimum during the first months of 2020 (specifically from January to April). Although the exact maximum point is not fully visible, as the curve does not show the characteristic peak, we selected the closest available observations from January and May 2022. Below, we present the Cross-Correlation Function (CCF) profiles of some spectra of HD 99797, which compare the observed spectra with a model-generated curve.

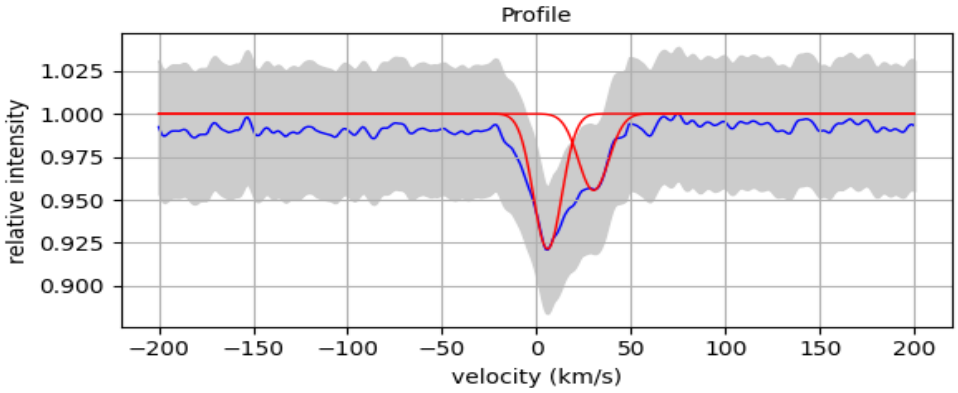

Figure 2. Graph of Cross-Correlation Function (CCF), HD 99797, Spectra: HD99797_R_2020_01_16_03_20_33.dat

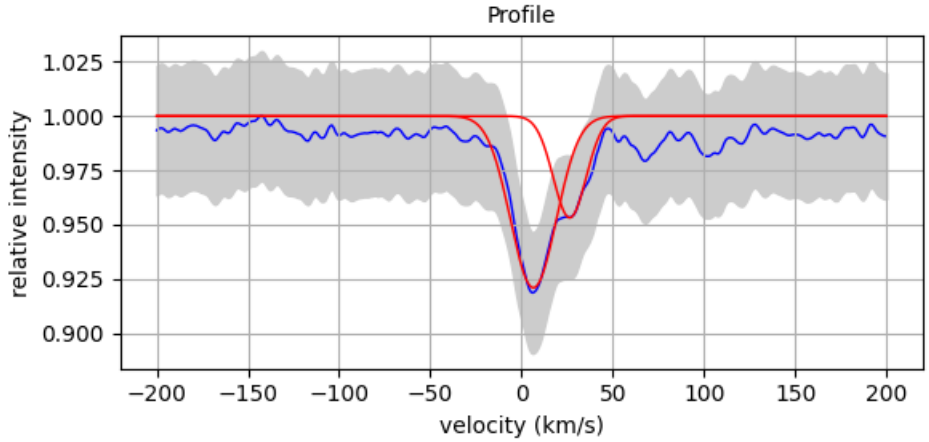

Figure 3. Graph of Cross-Correlation Function (CCF), HD 99797, Spectra: HD99797_R_2020_01_28_03_28_32.dat

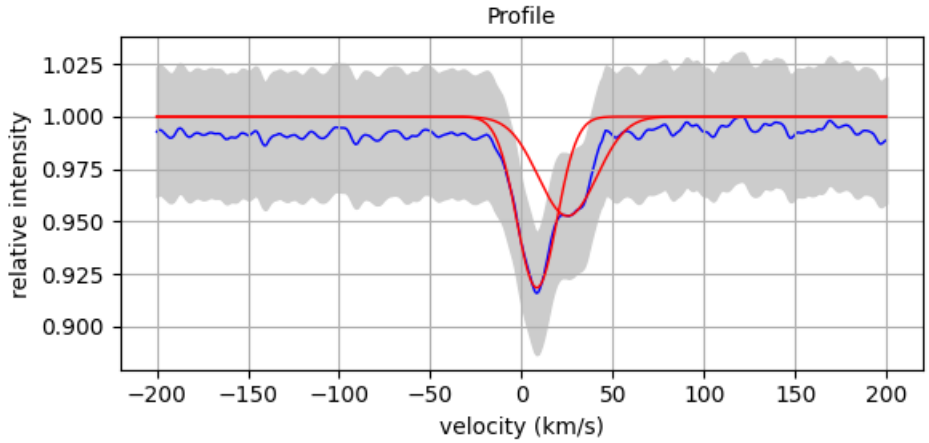

Figure 4. Graph of Cross-Correlation Function (CCF), HD 99797, Spectra: HD99797_R_2020_02_10_03_06_20.dat

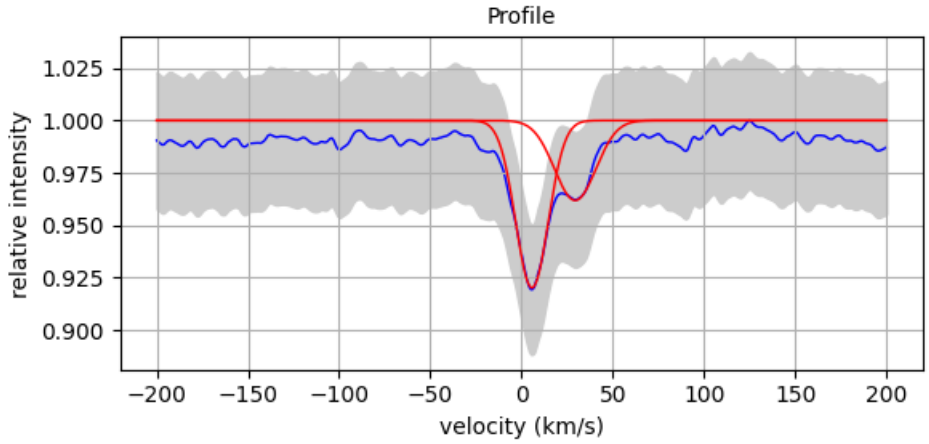

Figure 5. Graph of Cross-Correlation Function (CCF), HD 99797, Spectra: HD99797_R_2020_04_11_23_29_36.dat

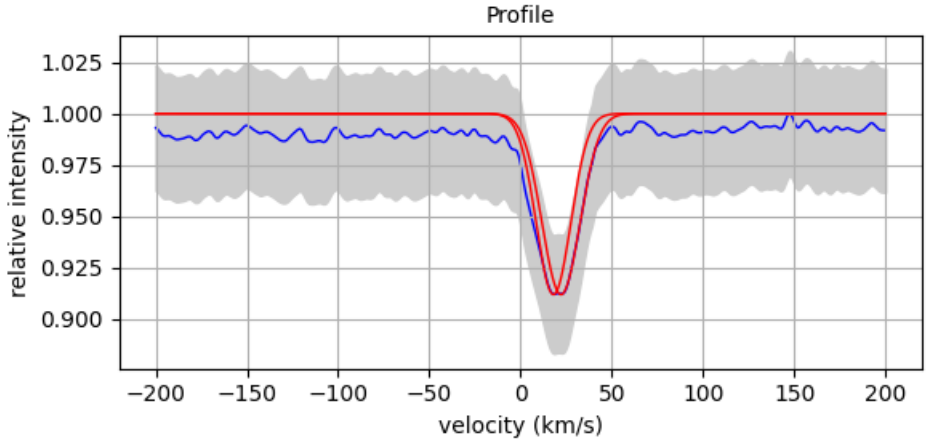

Figure 6. Graph of Cross-Correlation Function (CCF), HD 99797, Spectra: HD99797_R_2022_01_18_06_39_25.dat

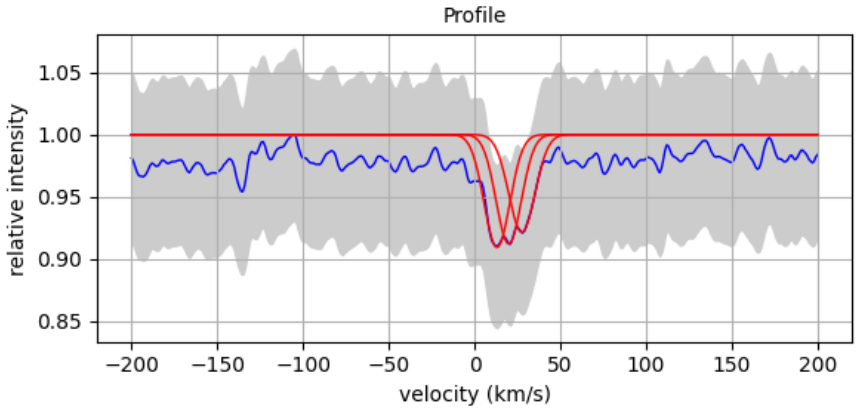

Figure 7. Graph of Cross-Correlation Function (CCF), HD 99797, Spectra: HD99797_R_2022_05_01_02_41_17.dat

VOLUMEN 48
XXXI Verano De la Ciencia
ISSN 2395-9797
www.jovenesenlaciencia.ugto.mx

Figures 2 to 7 show the radial velocity of the primary star of HD 99797 and signatures of what appears to be the secondary component. It is important to note that the most pronounced dip corresponds to the primary star, while the weaker signal represents the secondary star. The data from the 2020 observations are quite similar to each other, whereas the 2022 data show an abrupt change, both in velocity and in the shape of the curves, as expected from the orbital phases discussed earlier. For a more precise analysis, the parameters extracted from each CCF were compiled in Table 4. This allowed us to study the data using a comparison table, making it easier to perceive the overall characteristics of the graphs together.

***Table 4**. Parameters of the star HD 99797 in the maximum points and minimum points of radial velocity.*

Spectra	*Primary Star Vrad (km s⁻¹)*	*FWHM (km s⁻¹)*	*Secondary Star Vrad (km s⁻¹)*	*FWHM (km s⁻¹)*
HD99797_R_2020_01_16_03_20_33.dat	5.87±0.24	7.51	30.20±0.57	8.01
HD99797_R_2020_01_28_03_28_32.dat	8.25±0.26	10.96	25.19±0.75	15.98
HD99797_R_2020_02_10_03_06_20.dat	6.47±0.39	12.50	26.37±0.62	8.97
HD99797_R_2020_04_11_23_29_36.dat	5.70±0.26	8.62	29.38±0.77	11.33
HD99797_R_2022_01_18_06_39_25.dat	18.03±0.62	9.46	22.18±0.37	10.38
HD99797_R_2022_05_01_02_41_17.dat	13.15±0.28	7.51	20.01±0.18	7.36

Finally, we note that the Full Width at Half Maximum (FWHM) values for both stars fall within a similar range. For the primary star, the FWHM varies between 7.5 and 12.5 km s^{-1}, while for the secondary component, it ranges from 7 to 16 km s^{-1}. Additionally, we observed that this parameter changes depending on the specific spectrum being analyzed, showing clear variations based on whether the system is at a maximum or minimum velocity point.

Discussion Of The Results

The general properties we initially established from the results are essential for better understanding binary systems. One of the characteristics used to confirm that these are indeed binary systems is the presence of very large variations of their radial velocities. This high variation indicates that the measured radial velocity of the stellar system is being affected by the star orbiting a shared center of mass. The measured radial velocity changes depending on where the star is in its inner binary orbit, which explains why this prominent difference arises. Therefore, radial velocity is a property of great interest for determining further parameters of the secondary star.

In the second part of the results, we searched for objects close to the primary star. From Table 2, we observe that Gaia only detected nearby objects for HD 195543, HD 32575, and HD 189985, and we only have parallax and brightness for one of these stars. This brightness parameter is between 12 and 18 mag. According to the Pogson scale, the star close to our primary is very faint. This is lower than expected for a secondary star, given that the brightness of the primary star is much higher (in the range of 6-7 mag, as seen in Table 1). Thus, these are not detections of the secondary star.

The analysis of the spectra may provide more precise information about the secondary star. As observed, from our sample of 39 targets, only one system could be fully analyzed. This is because, when analyzing the remaining 38 targets using iSpec (Blanco-Cuaresma, 2019), the signal of the secondary star could not be found in the Cross-Correlation Function (CCF) profiles of the radial velocities. For the star HD 99797, even though its period mapping covers the years 2018 to 2024, there is not much data during its maximum and minimum points, as shown in Figure 1. However, the spectra obtained by TIGRE (Schmitt *et al.,* 2014) allowed us to capture information about the secondary star; that is, they clearly show the double spectral lines of the binary system, as shown in Figures 2 to 7.

Figures 2 to 5 correspond to the minimum points of the radial velocity curve (Figure 1), with an amplitude of approximately -12.3 km s^{-1}. Given that the perceived systemic radial velocity is 16.01 km s^{-1} (Table 1), the predicted relative radial velocity in the CCF would be 3.71 km s^{-1}. Table 4 shows the radial velocity of these minimum points. Note that the velocity of the primary star ranges from 5.70 km s^{-1} to 18.03 km s^{-1}, which is slightly above the predicted value. However, this discrepancy can be attributed to instrumental errors during the capture of the spectra by the telescope. The measured velocities for the secondary star are 30.20 km s^{-1}, 25.19 km s^{-1}, 26.37 km s^{-1}, and 29.38 km s^{-1}. There is significant scatter, making it difficult to clearly determine the exact radial velocity, although we now have a study range to approximate it.

Finally, Figures 6 and 7 correspond to the maximum points of the radial velocity curve (Figure 1), with an amplitude of approximately 3 km s^{-1}. While the systemic radial velocity is 16.01 km s^{-1} (Table 1), the predicted velocity should be 19.01 km s^{-1}. According to the data in Table 4, we have values of 13.15 km s^{-1} and 18.03 km s^{-1}. Although these measurements do not perfectly match the prediction, one of them is very close to the expected value. For the secondary star, we have radial velocities of 22.18 km s^{-1} and 20.01 km s^{-1}. These are on the wrong side of the primary's values. Since the primary is at the maximum, the secondary should be at the minimum and have lower Vrad. This is not the case. Thus, these measurements of the secondary radial velocity are not reliable.

Conclusions

Identifying double-lined spectroscopic binaries (SB2) is an observationally challenging task. As demonstrated in this study, detecting the secondary star is highly complex; from our initial sample of 39 candidates, only one system (HD 99797) exhibited clear double-line characteristics in its Cross-Correlation Function (CCF) profiles of the radial velocity. The secondary components in the CCF allowed us to extract radial velocity information for this star. Although the current data did not allow us to determine the radial velocity with absolute precision, we successfully constrained this parameter to a specific range, between 20.01 km s^{-1} and 30.20 km s^{-1}.

The double spectral lines detected in this study provide a foundational starting point for determining the fundamental parameters of the secondary star. Future research will be able to refine this information and derive additional parameters by acquiring more spectra over the coming years using the TIGRE telescope. Furthermore, a more rigorous analysis can be performed by utilizing advanced tools within iSpec, as well as by conducting detailed studies of X-ray emission and the line widths of the velocity curves.

References

Blanco-Cuaresma, S. (2019). Modern stellar spectroscopy caveats. *Monthly Notices of the Royal Astronomical Society*, *486*(2), 2075–2101. https://doi.org/10.1093/mnras/stz549

Blanco-Cuaresma, S., Soubiran, C., Heiter, U., & Jofré, P. (2014). Determining stellar atmospheric parameters and chemical abundances of FGK stars with iSpec. *Astronomy & Astrophysics*, *569*, A111. https://doi.org/10.1051/0004-6361/201423945

Carroll, B. W. . (2014). *An introduction to modern astrophysics*. Pearson.

Jack, D., Hernández Huerta, M. A., Rosas-Portilla, F. D., & Schröder, K. (2022). Bright spectroscopic binaries: II. A study of five systems with orbital periods of days. *Astronomische Nachrichten*, *343*(3). https://doi.org/10.1002/asna.20210015

Jack, D., Hernández Huerta, M. A., Rosas-Portilla, F. D., & Schröder, K. (2024). Bright spectroscopic binaries: III. Binary systems with orbital periods of P < 500 days. *Astronomische Nachrichten*, *345*(1). https://doi.org/10.1002/asna.20230123

Jack, D., Hernández Huerta, M. A., Rosas-Portilla, F., & Schröder, K. (2026). Bright Spectroscopic Binaries: IV. Additional Binary Systems With P<1000 Days. *Astronomische Nachrichten*, *347*(3). https://doi.org/10.1002/asna.70076

Jack, D., Hernández Huerta, M. A., & Schröder, K. (2020). Bright spectroscopic binaries: I. Orbital parameters of five systems with periods of P < 365 days. *Astronomische Nachrichten*, *341*(6–7), 616–627. https://doi.org/10.1002/asna.202013741

Merloni, A., Lamer, G., Liu, T., Ramos-Ceja, M. E., Brunner, H., Bulbul, E., Dennerl, K., Doroshenko, V., Freyberg, M. J., Friedrich, S., Gatuzz, E., Georgakakis, A., Haberl, F., Igo, Z., Kreykenbohm, I., Liu, A., Maitra, C., Malyali, A., Mayer, M. G. F., … Zheng, X. (2024). The SRG/eROSITA all-sky survey. *Astronomy & Astrophysics*, *682*, A34. https://doi.org/10.1051/0004-6361/202347165

Pattnaik, S., Kamila, S. K., Roy, G. S., Nayak, M. K., Das, R., & Sharma, N. K. (2011). Binary Star System-A Spectral Analysis. *Am. J. Phys. Educ*, *5*(2), 438. http://www.lajpe.org

Predehl, P., Andritschke, R., Arefiev, V., Babyshkin, V., Batanov, O., Becker, W., Böhringer, H., Bogomolov, A., Boller, T., Borm, K., Bornemann, W., Bräuninger, H., Brüggen, M., Brunner, H., Brusa, M., Bulbul, E., Buntov, M., Burwitz, V., Burkert, W., … Yaroshenko, V. (2021). The eROSITA X-ray telescope on SRG. *Astronomy & Astrophysics*, *647*, A1. https://doi.org/10.1051/0004-6361/202039313

Prusti, T., de Bruijne, J. H. J., Brown, A. G. A., Vallenari, A., Babusiaux, C., Bailer-Jones, C. A. L., Bastian, U., Biermann, M., Evans, D. W., Eyer, L., Jansen, F., Jordi, C., Klioner, S. A., Lammers, U., Lindegren, L., Luri, X., Mignard, F., Milligan, D. J., Panem, C., … Zschocke, S. (2016). The *Gaia* mission. *Astronomy & Astrophysics*, *595*, A1. https://doi.org/10.1051/0004-6361/201629272

Schmitt, J. H. M. M., Schröder, K. -P., Rauw, G., Hempelmann, A., Mittag, M., González-Pérez, J. N., Czesla, S., Wolter, U., Jack, D., Eenens, P., & Trinidad, M. A. (2014). TIGRE: A new robotic spectroscopy telescope at Guanajuato, Mexico. *Astronomische Nachrichten*, *335*(8), 787–796. https://doi.org/10.1002/asna.201412116

Vallenari, A., Brown, A. G. A., Prusti, T., de Bruijne, J. H. J., Arenou, F., Babusiaux, C., Biermann, M., Creevey, O. L., Ducourant, C., Evans, D. W., Eyer, L., Guerra, R., Hutton, A., Jordi, C., Klioner, S. A., Lammers, U. L., Lindegren, L., Luri, X., Mignard, F., … Zwitter, T. (2023). *Gaia* Data Release 3. *Astronomy & Astrophysics*, *674*, A1. https://doi.org/10.1051/0004-6361/202243940

Voges, W., Aschenbach, B., Boller, T., Bräuninger, H., Briel, U., Burkert, W., Dennerl, K., Englhauser, J., Gruber, R., Haberl, F., Hartner, G., Hasinger, G., Kürster, M., Pfeffermann, E., Pietsch, W., Predehl, P., Rosso, C., Schmitt ⋆⋆⋆, J. H. M. M., Trümper, J., & Zimmermann, H. U. (1999). *The ROSAT All-Sky Survey Bright Source Catalogue*. http://wave.xray.mpe.mpg.de/rosat/catalogues/rass-bsc.1

Wenger, M., Ochsenbein, F., Egret, D., Dubois, P., Bonnarel, F., Borde, S., Genova, F., Jasniewicz, G., Laloë, S., Lesteven, S., & Monier, R. (2000). The SIMBAD astronomical database. *Astronomy and Astrophysics Supplement Series*, *143*(1), 9–22. https://doi.org/10.1051/aas:2000332